Available online at www.sciencedirect.com
ScienceDirect
Catalysis Communications 9 (2008) 1201–1208
CATALYSIS COMMUNICATIONS
www.elsevier.com/locate/catcom

Study of CuCoZnAl oxide as catalyst for the hydrogen production from ethanol reforming

Agustín E. Galetti [a], Manuel F. Gomez [a], Luis A. Arrua [a], Alberto J. Marchi [b], Maria Cristina Abello [a,*]

[a] INTEQUI, (UNSL-CONICET), Instituto de Investigaciones en Tecnología Química, Chacabuco y Pedernera, 5700 San Luis, Argentina
[b] INCAPE (FIQ-UNL-CONICET), Santiago del Estero 2654, 3000 Santa Fe, Argentina

Received 27 June 2007; received in revised form 9 October 2007; accepted 5 November 2007
Available online 23 November 2007

Abstract

Ethanol steam reforming was studied over CuCoZnAl oxide with the addition of potassium. The catalyst was prepared by the coprecipitation method and characterized by X-ray diffraction, thermogravimetry, Raman spectroscopy, temperature programmed reduction, BET specific surface area and SEM-EDAX. The influence of reaction temperature was examined between 400 and 600 °C with a H_2O/C_2H_5OH molar ratio of 3.8. At 600 °C, the catalyst was very active with an ethanol conversion of 100%. The main products were CO_2 and CO and minor amounts of CH_4. The hydrogen yield was 5.2 mol of H_2 per mol of ethanol, which means a high hydrogen selectivity (87%). Stable activity and selectivity were obtained at 600 °C which could be attributed to the removing of carbonaceous deposits.

Keywords: Ethanol reforming; Hydrogen production; Mixed oxide catalyst

1. Introduction

In recent years, as a consequence of the foreseen reduction in fossil resources and environmental constraints, a great interest for new energy sources has been shown. The hydrogen has been pointed out as the alternative fuel, and the scientific community has oriented a lot of research works to the generation, storage and transportation of hydrogen. Different raw material and reactions have been proposed to the hydrogen production. In this sense, ethanol from biomass has a great potential not only because the renewable origin but also for its rich hydrogen content. According to the ethanol steam reforming reaction

$$C_2H_5OH + 3H_2O \rightarrow 6H_2 + 3CO_2$$

a maximum yield of six moles of hydrogen for each mol of ethanol could be obtained. However, many side reactions leading to the production of rich hydrogen compounds like CH_4, C_2H_4O, C_3H_6O, C_2, C_3 reduce the expected hydrogen yield. Besides, some of these compounds act as coke precursors leading to the formation of carbonaceous deposits. The development of an active, highly selective and very stable catalyst has become one of the keys in the hydrogen production. Different catalytic systems based on Cu, Co, Ni, Cu–Ni and Cu–Co oxides, with and without alkaline addition, [1–13] have shown to be active for ethanol reforming with variables hydrogen selectivities. The support seems to play an important role in the steam reforming reaction: (i) it should favour water splitting into OH groups and promote their migration to the metal particles; (ii) it should promote the dehydrogenation route for decreasing the deactivation by coke; and (iii) it should contribute to the stabilization of the metal particles at high temperature under steam [14]. Aluminium spinels seem to be a good option as catalytic supports. They are stable

* Corresponding author. Tel./fax: +54 2652 426711.
E-mail address: cabello@unsl.edu.ar (M.C. Abello).

1566-7367/$ - see front matter © 2007 Elsevier B.V. All rights reserved.
doi:10.1016/j.catcom.2007.11.015

under reforming conditions, mechanically resistant and present a low surface acidity [15]. When ternary Cu/Co(Zn)/Al oxides were prepared by coprecipitation method the formation of spinels was detected [16–18]. As far as we known the catalytic system CuCoZnAl has not been examined in the ethanol steam reforming. In this work the results of the synthesis, characterization, activity and stability of a CuCoZnAl catalyst modified by the K are reported.

2. Experimental

The catalyst was prepared by coprecipitation method from an aqueous solution of the metal nitrates with K_2CO_3 at 60 °C and pH = 7 in a stirred batch reactor [18]. After precipitation, the solid was collected by filtering and washed with hot (90 °C) distilled and deionzed water (400 ml). This washing step was carried out in order to partially remove K content. Then, the solid was dried overnight at 70 °C and finally underwent a decomposition process at a final temperature of 500 °C for 480 min. The decomposition was carried out under N_2 flow (30 ml min^{-1}) by using a temperature program which was determined from TGA experiment of the precursor. The Cu and Co nominal loading was fixed to 12 wt.% and the molar ratio Zn:Al = 0.5. The chemical composition of catalyst was confirmed by atomic absorption spectroscopy.

The BET surface area was measured by using a Micromeritics Accusorb 2100E instrument by adsorption of nitrogen at −196 °C. XR diffraction patterns (XRD) were obtained with a RIGAKU diffractometer operated at 30 kV and 20 mA by using Ni-filtered Cu Kα radiation ($\lambda = 0.15418$ nm) at a rate of 3 °C min^{-1} from $2\theta = 10°$ to 80°. The TG analyses were recorded by using TGA 51 Shimadzu equipment. The sample was heated from room temperature to 1000 °C at 10 °C min^{-1} with a N_2 (or air) flow of 50 ml min^{-1}. Scanning electron micrographs were obtained in a LEO 1450 VP. This instrument is equipped with an energy dispersive X-ray microanalyzer, EDAX Genesis 2000 with Si(Li) detector, which permitted analytical electron microscopy measurements. The samples were sputter coated with gold. The Raman spectra were run with a JASCO TRS-600SZ-P equipped with a CCD detector. The samples were excited with the 514 nm Ar line and the spectra acquisition consisted of five accumulations of 180 s for each sample. The reducibility was studied by hydrogen temperature programmed reduction (TPR) in a conventional equipment. The sample was pretreated in He at 300 °C for 60 min, cooled at 25 °C and reduced a 30 ml min^{-1} flow of 5 vol% H_2 in N_2, from 25 to 700 °C at a rate of 5 °C min^{-1}, and held at 700 °C for 2 h. Hydrogen consumption was monitored by a thermal conductivity detector after removing the water formed.

The ethanol steam reforming reaction was carried out in a fixed-bed quartz tubular reactor operated at atmospheric pressure. The reaction temperature was measured with a coaxial thermocouple. The feed was a gas mixture of ethanol, water and helium. Ethanol and water were fed through independent saturators before mixing. The flow rate was 70 ml min^{-1} at room temperature with an ethanol molar composition of 3%. The H_2O:C_2H_5OH molar ratio was 3.8 in all the experiments. The catalyst weight was 300 mg (0.3–0.4 mm particle size). The catalyst was heated to the reaction temperature under He flow, then the mixture with $C_2H_5OH + H_2O$ was allowed to enter into the reactor to carry out the catalytic test. In all the cases fresh samples were used. The reactants and reaction products were analyzed on-line by gas chromatography. H_2, CH_4, CO_2 and H_2O were separated by a 1.8 m Carbosphere (80–100 mesh) column and analyzed by TC detector. Nitrogen was used as an internal standard. Besides, CO was analyzed by a flame ionization detector after passing through a methanizer. Higher hydrocarbons and oxygenated products (C_2H_4O, C_2H_4, C_3H_6O, C_2H_5OH, etc) were separated in RT-U PLOT capillary column and analyzed with FID using N_2 as carrier gas. The homogeneous contribution was tested with the empty reactor. These runs showed no activity at 500 °C whereas the ethanol conversion was 3% at 600 °C being acetaldehyde the only product.

Ethanol conversion, selectivity to products and yield to hydrogen were defined as

$$X_{\mathrm{EtOH}} = \frac{F^{\mathrm{in}}_{\mathrm{EtOH}} - F^{\mathrm{out}}_{\mathrm{EtOH}}}{F^{\mathrm{in}}_{\mathrm{EtOH}}} 100$$

$$S_i = \frac{v_i F^{\mathrm{out}}_i}{2(F^{\mathrm{in}}_{\mathrm{EtOH}} - F^{\mathrm{out}}_{\mathrm{EtOH}})} 100$$

$$Y_{\mathrm{H2}} = \frac{F^{\mathrm{out}}_{\mathrm{H2}}}{F^{\mathrm{in}}_{\mathrm{EtOH}}}$$

Being F^{in}_i and F^{out}_i the molar flow rates of product "i" at the inlet and outlet of the reactor and v_i the number of carbon atoms in "i".

3. Results and discussion

Table 1 summarizes some characteristics of the catalyst. It can be observed that the achieved compositions are in good agreement with nominal ones. XRD patterns are shown in Fig. 1. The precursor shows a crystalline hydrotalcite phase, Fig. 1a, which is completely decomposed after the thermal treatment. The diffraction pattern of final solid after decomposition reveals broad peaks at values of 2θ which could be corresponded to different spinel phases: $ZnAl_2O_4$, $CoAl_2O_4$, Co_3O_4, Fig. 1b. Complementary studies (shown forward) indicate that those peaks mainly corre-

Table 1
Chemical composition and specific surface area of CuCoZnAl catalyst after N_2 decomposition

	Co	Cu	Zn	Al	S_{BET} ($m^2\ g^{-1}$)
Nominal composition (wt.%)	11.3	12.2	25.1	20.7	34
Actual content (wt.%)	9.8	13.8	n.d.	20.1	

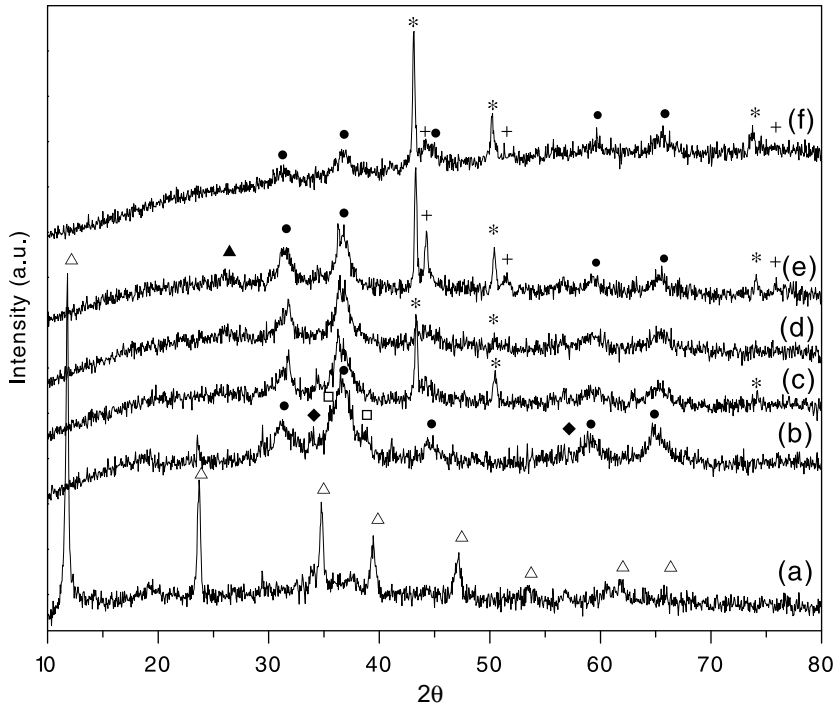

Fig. 1. Diffraction patterns of CuCoZnAl catalyst (a) precursor; (b) fresh sample; after being used in reaction at (c) 400 °C, (d) 500 °C and (e) 600 °C; (f) after TPR experiment in H_2. Δ hydrotalcite; ● $ZnAl_2O_4$; ♦ CoO; □ CuO; + Co; ∗ Cu; ▲C.

spond to $ZnAl_2O_4$. Weak peaks at $2\theta = 38.7°$, 35.5° (JCPDS-41-254) and 34.1°, 57.3° (JCPDS-42-1300) corresponding to CuO and CoO, respectively are also observed. No peaks attributed to potassium crystalline are detected. Co^{+3} compounds cannot be ruled out from the XRD. Similar conclusions can be reached from Raman spectroscopy. In Fig. 2a the spectrum for the fresh sample is shown. Broad bands in the region between 400 and 700 cm^{-1} are

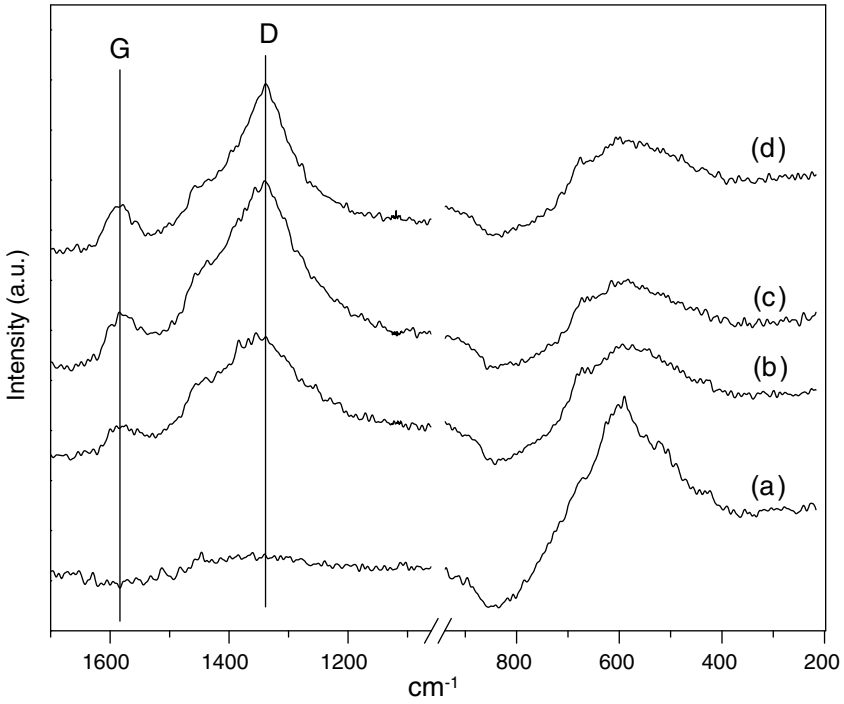

Fig. 2. Raman spectra of CuCoZnAl catalyst after different treatments. Fresh sample; (a) after being used in reaction at (b) 400 °C and 300 min; (c) 500 °C and 180 min; (d) 600 °C and 1060 min.

observed, which corresponds to the active modes for $ZnAl_2O_4$, $CoAl_2O_4$, Co_3O_4 and CoO [19,20]. In literature, it is reported that the decomposition of hydrotalcite precursor in N_2 favors the Co^{+2} compound formation and prevents the formation of Co_3O_4 [18]. This discrepancy could be an indication that the N_2 flow during decomposition was not completely O_2-free. The presence of Co_3O_4 and/or $CoAl_2O_4$ can be formed under mild oxidizing conditions [18].

The reducibility of the sample was studied by temperature programmed reduction. The TPR profile illustrated in Fig. 3 shows two bands of H_2 consumption. The 89% of reducible species reduces in the temperature range between 200° and 430 °C, with peaks centered at 357° and 371 °C. The first band could be assigned to the reduction of Cu^{+2} to Cu^0 and Co^{+2}/Co^{+3} to Co^0. The reduction temperature for Cu^{+2} species is higher than the obtained for pure CuO. This behavior could be a consequence of potassium presence or an indication of strong interactions Cu–Co or the presence of Cu–Co compounds. The formation of these compounds has been reported in literature and involves the coexistence of Co species in tetrahedral and octahedral coordination with differences in reducibility. The second band between 430° and 730 °C with a maximum at 520 °C, represents 11% of H_2 consumption. It can be associated to the reduction of Co^{+2} strongly interacted with $ZnAl_2O_4$ or forming $CoAl_2O_4$. The total H_2 consumption is higher than the required if all Co species were as Co^{+2}; then it could be inferred that a fraction of Co is as Co^{+3}. The XRD of the reduced sample after TPR experiment, Fig. 1f, reveals the presence of metallic copper and weak peaks at $2\theta = 44.2°$, 51.5° and 75.8° corresponding to Co^0. From these results an important sintering of copper particles can be observed whereas cobalt particles remain highly dispersed. The peaks at $2\theta = 36.9°$, 31.3°, 59.4° and 65.3° are attributed to $ZnAl_2O_4$ which is not reduced under the TPR conditions [21].

The mixed oxide, without a previous reduction, was tested in the ethanol reforming reaction. In Fig. 4a the catalytic results obtained at 400 °C are shown. The ethanol conversion decreases from an initial value nearly to 100% to 35% at 300 min of time on stream. The H_2 yield also decreases from 3.5 to 1.4 mol of H_2 per mol of ethanol fed. The main products are CO_2, C_2H_4O, C_3H_6O and CO. In addition, the formation of CH_4 and C_3 is also detected in small amounts. After 300 min of time on stream, an increase of pressure is observed into the reactor and the effluent flow decreases by 30%. This effect is more

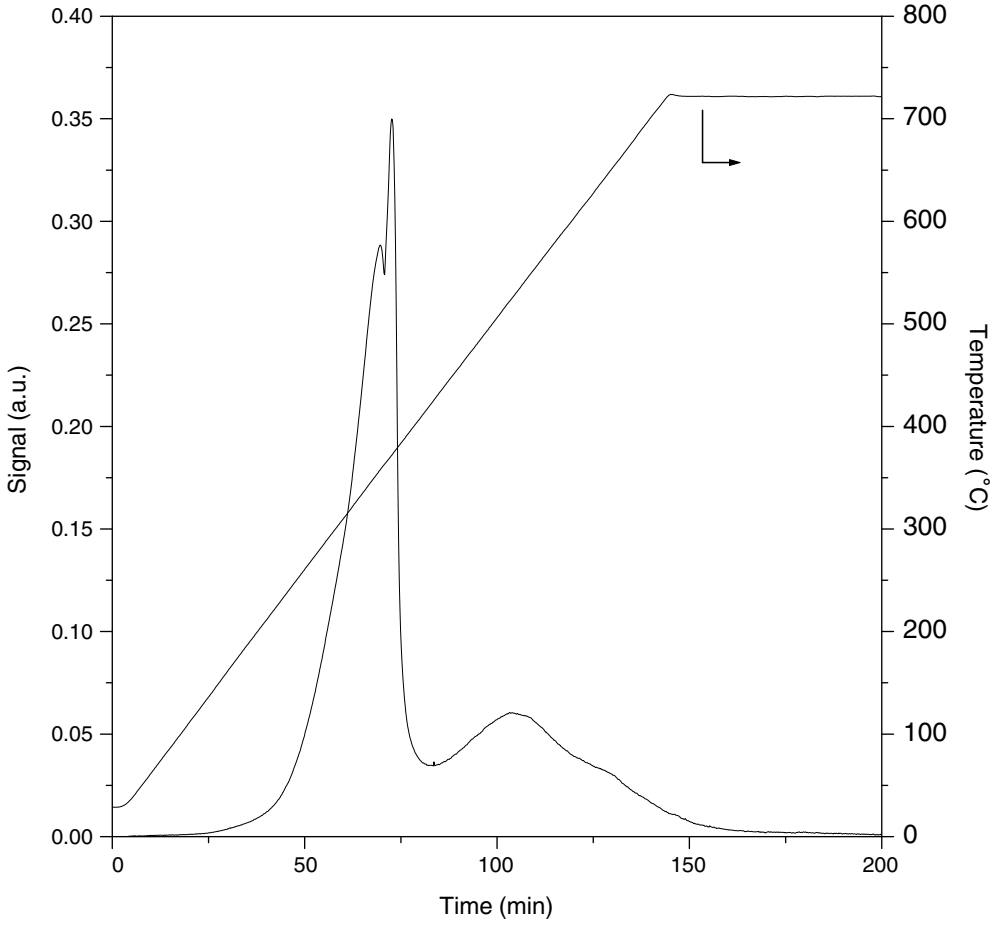

Fig. 3. Temperature programmed reduction profile for CuCoZnAl catalyst.

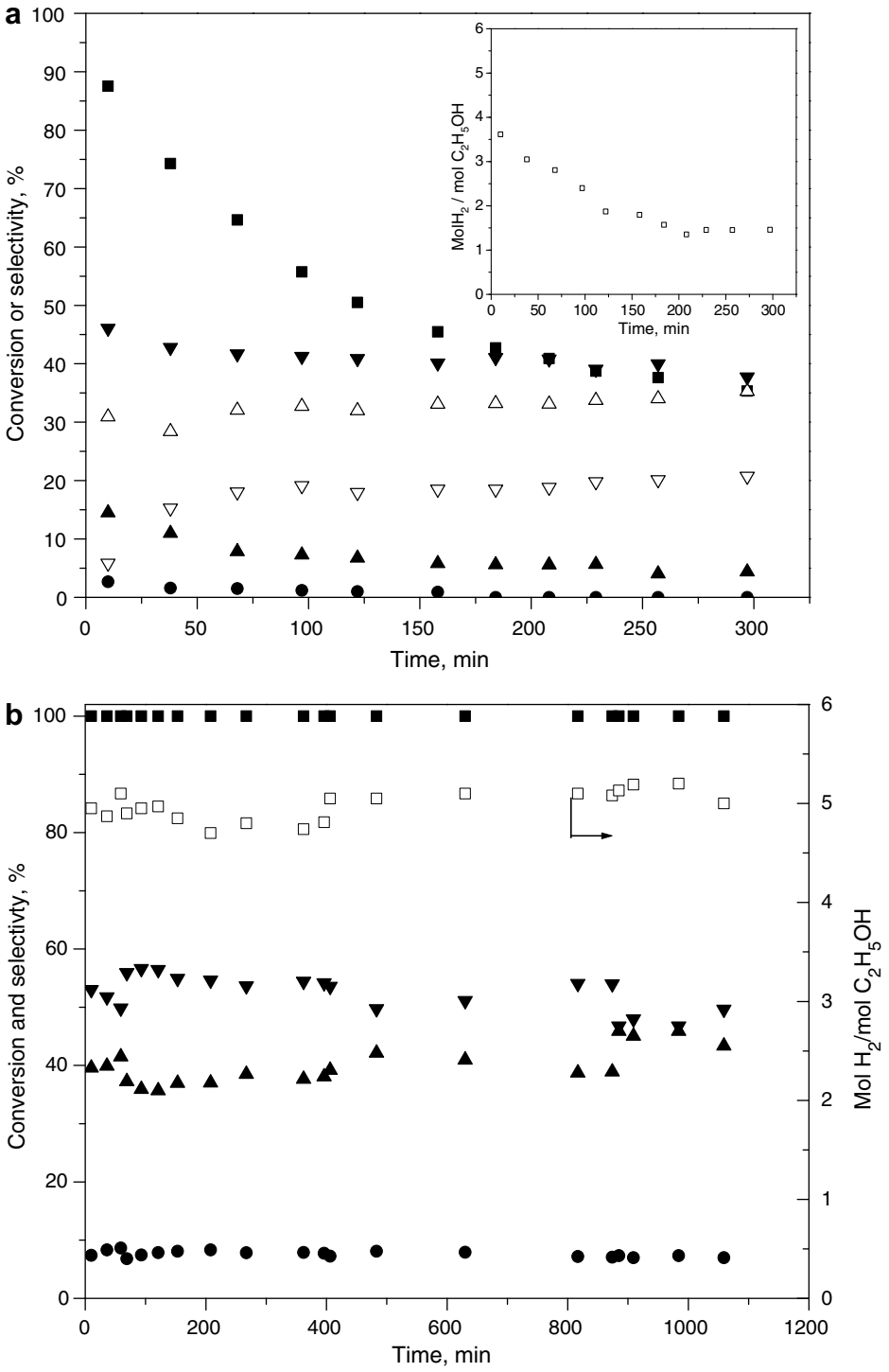

Fig. 4. (a) Catalytic results in ethanol steam reforming at 400 °C. Ethanol conversion (■), selectivity to CO_2 (▼), CO (▲), CH_4 (●), C_2H_4O (Δ), C_3H_6O (∇) and H_2 (□). Reaction temperature: 400 °C. Molar ratio H_2O:C_2H_5OH = 3.8. (b) Catalytic results in ethanol steam reforming at 600 °C. Ethanol conversion (■), selectivity to CO_2 (▼), CO (▲), CH_4 (●) and H_2 (□). Reaction temperature: 600 °C. Molar ratio H_2O:C_2H_5OH = 3.8.

important when the reaction temperature is 500 °C. At this temperature the initial conversion of ethanol is 100% and the only products are H_2, CO_2, CO and CH_4. After 180 min in operation the experimental run should be stopped as a consequence of the total bed blocking. In both cases the appearance of the used catalyst is similar with a visible coke formation. In a previous work, it was shown that pure $ZnAl_2O_4$ is not inert in the ethanol steam reforming [22]. The aluminum spinel mainly promotes the grown chain to acetone with a hydrogen yield of 2.3 mol H_2/mol C_2H_5OH at 500 °C. The spinel showed a high thermal resistance under the same experimental conditions used in this

work with a negligible carbon formation. At the reaction temperature and due to the H_2 production the CuCoZnAl catalyst undergoes reduction under test. Then, it can be inferred that carbon is produced on Cu^0 and Co^0 particles. Carbon filaments have been observed on Co based catalysts [23].

In Fig. 4b, the catalytic results obtained at 600 °C are shown. The catalyst is very active with 100% of ethanol conversion during 1060 min of time on stream. The main products are CO_2 and CO and minor amounts of CH_4. The H_2 yield expressed as mol of H_2 per mol of ethanol in the feed is 5.2. The initial CO_2/CO molar ratio is 1.4 and slightly decreases with the reaction time. The activity stability is notable although a visual observation of catalytic bed suggests the coke formation. Llorca et al. have reported hydrogen yield near to 5.7 mol of H_2 per mol of ethanol over cobalt–ZnO-based catalysts doped by Na [11]. They observed total conversion of ethanol at 450 °C by using a water:ethanol molar ratio of 13:1 which markedly higher than the molar ratio used in this work. Besides, they found that the incorporation of sodium increased the resistance to deactivation. The best results were obtained with catalysts with 0.78% and 0.98% Na. On bimetallic catalysts Co–Cu, similar yield to H_2 were reported but using lower temperatures [12]. On these systems deactivation by coke was not reported.

Assuming that the active phase represents 23.6 wt.% (13.8 wt.% Cu and 9.8 wt.% Co) the hydrogen yield obtained over the CuCoZnAl catalyst is similar to that on Ni–$ZnAl_2O_4$ with an equivalent loading [21]. At 600 °C both samples show a good stability. However, the CO_2/CO ratio is higher over CuCoZnAl (1.4 against 0.7) which could indicate that this catalyst favors the conversion of produced CO into CO_2 through the water gas shift reaction.

The XRD of used catalyst, Fig. 1c, d and e reveal the presence on metallic particles of Cu and Co together with the reflection lines corresponding to $ZnAl_2O_4$. The possibility of alloying and the presence of metal oxides as well as metallic solid solutions cannot be ruled out. Holms et al. have reported alloy formation and mixed oxides at the microstructural level in bimetallic Co–Cu catalysts supported on ZnO after running the ethanol steam reforming reaction [12]. An incipient peak at $2\theta = 26.4°$ corresponding to graphitic carbon is also observed.

The nature and characteristics of carbon deposits are studied by Raman spectroscopy and temperature programmed oxidation experiments. In Fig. 2, the Raman

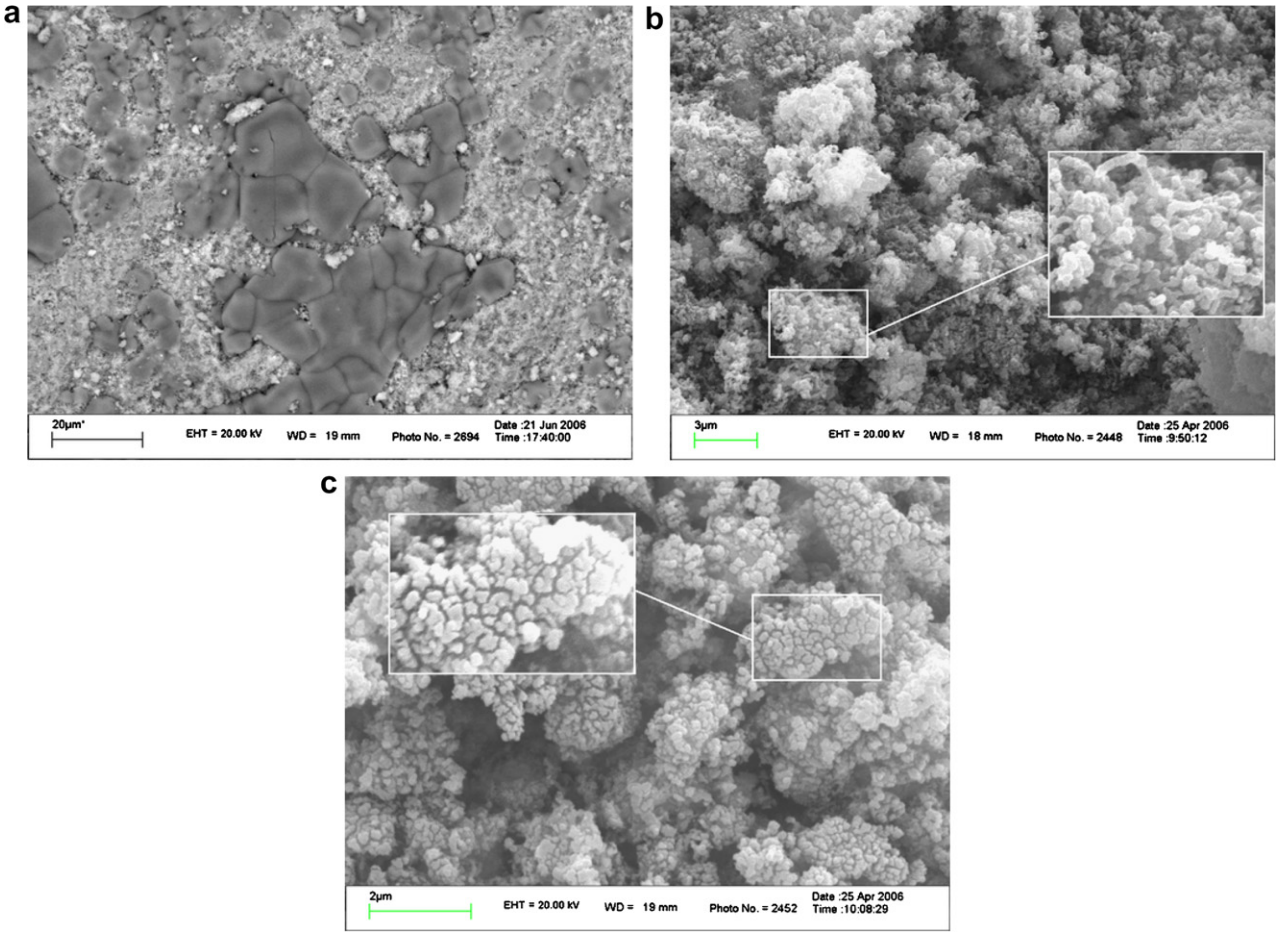

Fig. 5. SEM micrographs of (a) fresh sample (backscattering) and after being used in reaction at (b) 500 °C and 180 min and (c) 600 °C and 1060 min.

spectra of spent samples are shown in the range of 1000–1700 cm^{-1}. In all cases, two broad bands centered at 1593 cm^{-1} and 1350 cm^{-1} are observed which reveal the presence of ordered carbon, graphitic type, and disordered defective structures, respectively. The band at 1350 cm^{-1}, known as D band, is higher intensity than the band at 1593 cm^{-1}, known as G band. Then, a predominance of disordered structures such as amorphous carbon, nanoparticles of carbon or filamentous can be concluded [24]. In spite of having no differences in the carbon structures with the reaction temperature, differences in the relative intensity of the bands are observed. At 500 °C, the D band intensity is higher (it should be taken into account that the operation reaction time was 180 min whereas at 400 and 600 °C were 300 min and 1060 min, respectively) which means a higher coke formation; then, this could explain the reactor blocking in the experimental run. The intensity of broad band in the range of 400–700 cm^{-1} has decreased in agreement with the Co species reduction.

The formation of carbon deposit on the spent catalyst is also evidenced by SEM observations. In Fig. 5, the micrographs of fresh and spent catalysts are presented. The SEM micrograph for the fresh sample, Fig. 5a, shows particles of different morphology. The dark aggregates correspond to particles rich in potassium and the grey areas represent the zinc aluminate support with Co, Cu and K. The bulk chemical composition in K given by ICP was 0.77 wt.%. This value is markedly lower than the elemental composition given by EDAX in different particle zones. Then, it could be inferred that potassium is not homogeneously distributed. Significant changes in morphology are observed after reforming at different reaction temperatures, Fig. 5b and c. A well defined fibrous conformation clearly appears when the catalyst is used at 500 °C during 180 min of time on stream while a non-structured coke seems to be formed on the sample used at 600 °C.

The amount of carbon deposited on catalyst at each reaction temperature is determined by temperature programmed oxidation by means of thermogravimetry. Four zones of weight loss are clearly observed: up to 100 °C, between 100 and 470 °C, between 470 and 770 °C and after 770 °C. In all samples the weight constancy is not reached under the TG conditions. The first peak centered at 80 °C corresponds to water desorption; the second one, centered at 430 °C for the sample used at 400 and 500 °C and at 465 °C for the sample used at 600 °C, corresponds to the burning of amorphous carbon; and the third peak centered at 745 °C attributed to the burning of more ordered carbon [25,26]. Taking into account the total weight loss ($\Delta w\%$) between 100 and 1000 °C, the order is $\Delta w\%$ at 500 °C (17.4%) > $\Delta w\%$ at 400 °C (15.7%) > $\Delta w\%$ at 600 °C (13.7%) in agreement with the deactivation observed.

An analysis of catalytic results and those of post reaction characterization leads to the conclusion that the reaction temperature has an important effect in the coke deposition. When the catalyst is run at 600 °C under reforming conditions, a slight increase in CO selectivity in detriment to CO_2 selectivity is observed, Fig. 4b, without significant changes in H_2 yield. The characterization indicates changes in the extent of metallic species sintering, in particular of Cu^0 sinterized after being used at 400 and 600 °C. A growth of Co metallic particles is only observed

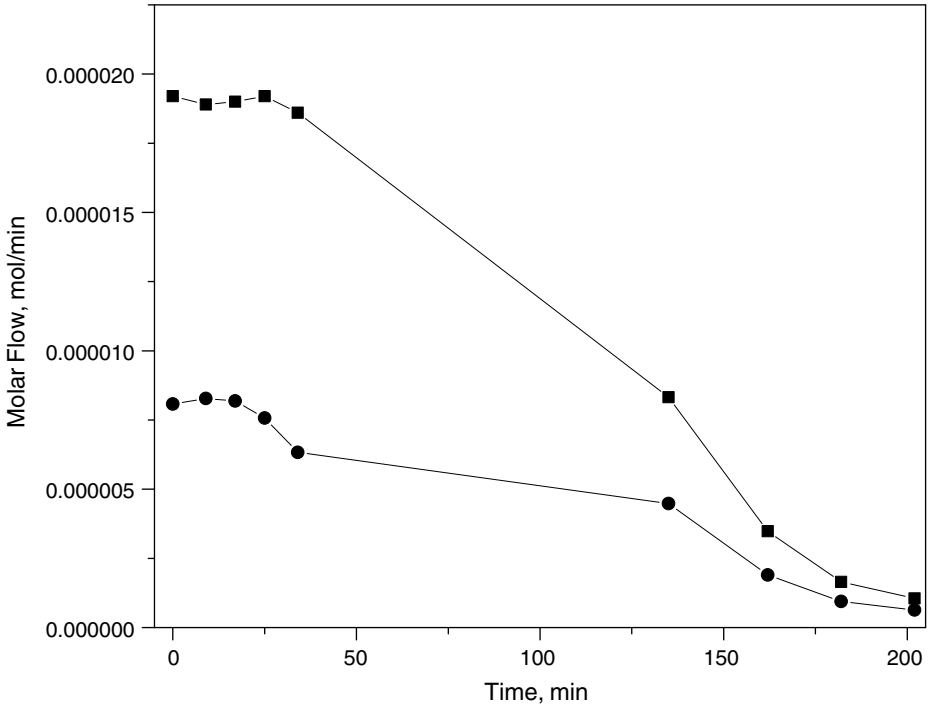

Fig. 6. Dynamic of the Boudouard reaction in CO_2 at 600 °C over spent CuCoZnAl catalyst. (●) CO; (■) CO_2.

at 600 °C probably by the presence of water [20], the high temperature and the long time under reaction. It calls the attention that the peaks of Cu^0 and Co^0 are incipient on sample used at 500 °C. Then, under the operation conditions used in this work, the sintering does not contribute in an important way to the deactivation phenomenon.

Raman spectroscopy reveals the formation of coke, predominantly amorphous, which could be removed from the catalyst surface by Boudouard reaction, according to the stoichiometric equation: $CO_2 + C_{(A)} = 2\ CO$, being $C_{(A)}$ amorphous carbon ($\Delta G^0_{600\ ^\circ C} = -4.4$ kJ mol^{-1}). The influence of this reaction in consuming carbon directly from the coke was checked by means of a complementary experiment. After using the catalyst at 600 °C for 300 min, the ethanol and water feed was interrupted and a CO_2 flow in helium was allowed to enter into the catalytic bed. The CO formation and CO_2 consumption were followed by chromatography and the results are shown in Fig. 6. After 210 min the formation of CO practically goes to zero and the CO_2 value recovers its initial composition. The experimental molar ratio CO_2/CO determined by integration of the curves (Fig. 5) is 0.42, which is near the 0.5 stoichiometric value. From this evidence it is reasonable to conclude that the simultaneous occurrence of Boudouard reaction at 600 °C improves the resistance to carbon deposition. At 400 and 500 °C the rate of coke deposition is higher than the removal rate and the catalytic bed is deactivated by carbon deposits. In fact, the Boudouard reaction is not thermodynamically favored at low temperatures. Besides, the presence of potassium on the catalyst surface positively affects the gasification of deposited carbon. An important catalytic effect of alkaline additives on the Boudouard reaction has been reported in literature [27–29].

4. Conclusions

Ethanol steam reforming reaction was studied over a quaternary mixed oxide CuCoZnAl with potassium adding. The preparation method led to the formation of spinel matrix mainly $ZnAl_2O_4$, with a high dispersion of oxidized species of Cu and Co. The catalyst was very active with 100% of ethanol conversion in the temperature range between 400 and 600 °C. After the reforming reaction two types of carbon structures were detected by Raman spectroscopy and SEM. Disordered carbon deposits were predominant in all reaction temperatures.

At 600 °C the hydrogen yield was 5.2 mol of H_2 per mol of ethanol fed and the stability of the catalyst was higher. Although the extent of sintering of metal particles of Cu^0 and Co^0 was high at this temperature the sintering does not contribute in an important way to the deactivation phenomenon. The simultaneous reactions of coking and carbon removal by Boudouard and gasification reactions improve the stability.

Acknowledgments

Financial supports are acknowledged to CONICET, ANPCyT and Universidad Nacional de San Luis. The authors wish to thank Dr. Beatriz Pierini (INCAPE) for Raman assistance.

References

[1] F. Auprete, C. Descorme, D. Duprez, Catal. Commun. 3 (2002) 263.
[2] V. Klouz, V. Fierro, P. Denton, H. Katz, J. Lisse, S. Bouvot-Mauduit, C. Mirodatos, J. Power Sources 105 (2002) 26.
[3] S. Freni, S. Cavallaro, N. Mondello, L. Spadaro, F. Frusteri, Catal Commun. 4 (2003) 259.
[4] F. Mariño, M. Boveri, G. Baronetti, M. Laborde, Int. J. Hydrogen Energy 29 (2004) 67.
[5] S. Cavallaro, V. Chiodo, S. Freni, N. Mondello, F. Frusteri, Appl. Catal. A: Gen. 249 (2003) 119.
[6] J. Sun, X. Qiu, F. Wu, W. Zhu, W. Wang, S. Hao, Int. J. Hydrogen Energy 29 (2004) 1075.
[7] A. Kaddouri, C. Mazzocchia, Catal. Commun. 5 (2004) 339.
[8] M. Batista, R. Santos, E. Assaf, J. Assaf, E. Ticianelli, J. Power Sources 124 (2003) 99.
[9] J. Llorca, N. Homs, J. Sales, P. Ramirez de la Piscina, J. Catal. 209 (2002) 306.
[10] F. Mariño, G. Baronetti, M. Jobbagy, Appl. Catal. A: Gen. 238 (2003) 41.
[11] J. Llorca, N. Homs, J. Sales, J.L.G. Fierro, P. Ramirez de la Piscina, J. Catal. 222 (2004) 470.
[12] N. Homs, J. Llorca, P. Ramirez de la Piscina, Catal. Today 116 (2006) 361.
[13] A.J. Vizcaíno, A. Carrero, J.A. Calles, Int. J. Hydrogen Energy 32 (2007) 1450.
[14] F. Aupretre, C. Descorme, D. Duprez, D. Casanave, D. Uzio, J. Catal. 233 (2005) 464.
[15] M.A. Valenzuela, J.P. Jacobs, P. Bosch, S. Reijne, B. Zapata, H.H. Brongersma, Appl. Catal. A 148 (1997) 315.
[16] M.F. Gomez, A.J. Marchi, M.C. Abello, in: Actas do XVII Simpósio Iberoamericano de Catálise, Porto, Portugal, 2000 p. 93.
[17] A.J. Marchi, PH thesis. Universidad Nacional del Litoral, Argentina, 1988.
[18] A.J. Marchi, J.I. Di Cosimo, C.R. Apesteguía, Catal. Today 15 (1992) 383.
[19] C.M. Fang, C.K. Loong, G.A. de Wijs, G. de Wuit, Phys. Rev. B 66 (2002) 144301.
[20] B. Jongsomijt, J. Panpranot, J. Goodwin, J. Catal. 204 (2001) 98.
[21] N. Barroso, M.F. Gomez, L.A. Arrúa, M.C. Abello, Appl. Catal. A: Gen. 304 (2006) 116.
[22] M.N. Barroso, M.F. Gomez, L.A. Arrúa, M.C. Abello, Catal. Lett. 109 (2006) 13.
[23] J.C. Vargas, S. Libs, A.-C. Roger, A. Kiennemann, Catal. Today 107–108 (2005) 417.
[24] F. Pompeo, N. Nichio, O. Ferretti, D. Resasco, Int. J. Hydrogen Energy 30 (2005) 1399.
[25] S. Natesakhawat, R. Watson, X. Wang, U.J. Ozkan, J. Catal. 234 (2005) 496.
[26] M.C. Sanchez-Sanchez, R.M. Navarro, J.L.G. Fierro, Int. J. Hydrogen Energy 32 (2007) 1462.
[27] W.H. Van Niekerk, R.J. Dippenaar, D.A. Kotze, J. S. Afr. Inst. Min. Metall. 86 (1986) 25.
[28] M. Demicheli, D. Duprez, J. Barbier, O. Ferretti, E. Ponzi, J. Catal. 145 (1994) 437.
[29] G. Chen, R.T. Yang, J. Catal. 138 (1992) 12.